establish a new experimental model system, to enable both macroscopic and histopathologic evaluation of KD-caused vascular lesions.

All aneurysmal lesions, whatever their etiology, share common pathologic hallmarks, including inflammation and proteolytic degradation of the extracellular matrix [13–16]. Excessive matrix proteolysis mediated by matrix metalloproteinases (MMPs), notably MMP-9, is considered a common and critical step during lesion development [13,15,17,18]. In fact, MMP-9 is upregulated in coronary lesions of the LCWE-induced mouse model [19] and also in patients with KD [20]. Inhibition of MMP-9 had been shown to prevent elastin degradation in the LCWE-induced mouse model, but it had no effect on inflammatory infiltration [19], which suggests that upstream signaling molecules would be a desirable target. We then focused on c-Jun N-terminal kinase (JNK), a stress-activated signaling molecule, which regulates MMP-9 and various proinflammatory cytokines [21,22]. SP600125, a specific JNK inhibitor, has been shown to completely block development of abdominal aortic aneurysm in mice, accompanied by reduction of MMP-9 and macrophage infiltration, and preservation of elastic lamellae [23].

We hypothesized that inhibiting JNK would attenuate development of vascular lesions in a mouse model of KD. Initially, we successfully created a mouse model system that allowed us to assess development of the lesions that are compatible with those in KD. Consequently, we showed that pharmacologic inhibition of JNK effectively prevented development of CAWE-induced lesions in mice.

2. Methods

2.1. CAWE preparation

Candida albicans cell wall extract (CAWE) was prepared from Candida albicans standard strain SC5314 by modifying the method described previously [9]. Briefly, Candida albicans SC5314 stock culture was stored at −80 °C, then incubated at 37 °C for 48 h aerobically on yeast peptone dextrose agar (10 g yeast extract, 20 g peptone, 20 g glucose and 20 g agar per liter). Yeast cells were harvested (about 600 mg wet weight/plate) from agar plates using a scraper and washed three times with distilled water. An extract was obtained by boiling yeast cells for 2 h with 0.5 M KOH (200 mg wet weight of yeast cells/ml). After alkali neutralization in pH7.2 and dialysis against water for 3 days, the extracted material was precipitated with ethanol. The precipitate, about 4% against wet weight yeast cells, was suspended in phosphate-buffered saline (PBS) and adjusted to a final concentration of 100 mg/ml.

2.2. Mice

Four-week-old C57BL/6 N male mice were purchased from Kyudo Co., Ltd. (Tosu, Saga, Japan). Mice were kept in plastic cages (5 per cage) under pathogen-free conditions in a room at 24±2.5 °C and 55%±5% relative humidity under a 12:12-h light–dark cycle. Mice were given free access to standard food and water throughout the experiments. All experiments were performed in conformity with the Guide for the Care and Use of Laboratory Animals published by the United States National Institutes of Health. The protocols were approved by the Laboratory Animal Care and Use Committee of Fukuoka University (#116479).

2.3. Induction of vascular lesions in mice

To induce vascular lesions, 4-week-old C57BL/6 male mice were injected intraperitoneally (i.p.) with 4 mg of CAWE for 5 consecutive days every 4 weeks for 2 cycles; and then euthanized with overdoses of sodium pentobarbital (100 mg/kg, i.p.) at 4, 8 or 12 weeks after the second CAWE cycle (Fig. 1A). For whole-body perfusion fixation, 4% paraformaldehyde in PBS was perfused at physiological pressure. After perfusion fixation, the hearts and the whole aortas with branches

were exposed and excised for morphometric and histological analyses. Additionally, in some experiments, a mixture of 10% India ink/4% gelatin in PBS was injected into aortic root to visualize coronary arteries.

2.4. Inhibition of JNK in mice

Custom-made pellets containing JNK-specific inhibitor SP600125 (30 mg/kg/day) and control placebo pellets were purchased from Innovative Research of America (Sarasota, FL, USA). For pellet implantation, 4-week-old C57BL/6 male mice were anesthetized with sodium pentobarbital (40 mg/kg, i.p.). Anesthesia was monitored by periodic observation of respiration and pain response. Pellets were implanted in subcutaneous pockets created on the backs of the mice before starting CAWE administration as described above. The mice were euthanized as described, at 4 weeks after the second CAWE cycle (Fig. 1B). After whole-body perfusion fixation as described, hearts and whole aortas with branches were excised, photographed for morphometric analysis, and analyzed histologically. Photographs of aortas were used to determine maximum external aortic diameters.

2.5. Histological and immunohistochemical analyses

Paraffin-embedded sections were stained with hematoxylin/eosin (HE) and elastica-van Gieson (EVG) for histological analysis. For EVG staining, sirius red was used instead of acid fuchsin. Sections were also probed with antibodies raised against appropriate antigens for immunohistochemistry, as described previously [24]. We detected tenascin-C (TN-C), α-smooth muscle actin (α-SMA), Mac-3 and activated JNK by probing sections with rabbit polyclonal anti-TN-C antibody [25], mouse anti-smooth muscle α-actin antibody (Dako, Glostrup, Denmark), rat anti-Mac-3 antibody (BD Biosciences, San Jose, CA, USA) and rabbit polyclonal anti-phosphorylated JNK (p-JNK) antibody (Promega, Fitchburg, WI, USA), respectively. The sections were visualized with an avidin–biotin–peroxidase complex staining kit (Vector Laboratories, Burlingame, CA, USA) and colorized with diaminobenzidine (DAB) chromogen. For double immunostaining, sections were incubated with anti-p-JNK antibody, visualized with a peroxidase complex staining kit and DAB, and incubated with fluorescein isothiocyanate-conjugated anti-α-SMA (Sigma, St. Louis, MO, USA) or anti-Mac-3 and Alexa Fluor 546 goat anti-rat IgG (Molecular Probes, Eugene, OR, USA). Slides were observed under a fluorescent/differential interference contrast (DIC) microscope (BH2, Olympus, Tokyo Japan). Immunofulorescent signals were superimposed on DIC images.

2.6. Statistical analysis

Data are expressed as mean±standard deviation (SD). Statistical analyses were performed with the Prism 5.0d statistical program (GraphPad Software, La Jolla, CA, USA). We used Fisher's exact test to compare incidence of aneurysm development. We used the Mann Whitney test to compare maximal aortic diameters between experimental groups. A value of P<0.05 was considered statistically significant.

3. Results

3.1. Development of arterial and aortic lesions induced by CAWE

To create a mouse model of KD-related lesions, we injected into 4-week-old C57BL/6 male mice with 4 mg of CAWE for 5 consecutive days for 2 cycles. Four to 12 weeks later, we found that a considerable number of mice developed bulging lesions and that these lesions were created at abdominal aorta, iliac artery, coronary artery, carotid artery, and celiac artery (Fig. 2A-D). Some mice had multiple lesions with a "string of beads" appearance (Fig. 2D). All of the lesions looked pearly white, which indicated that they were
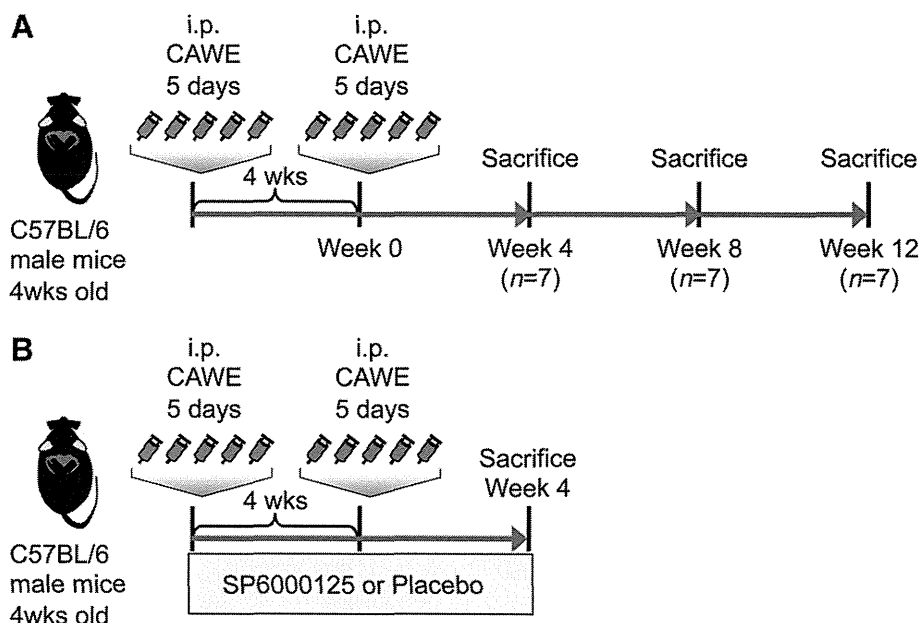
Fig. 1. Experimental design. A: To develop a mouse model of Kawasaki disease, *Candida albicans* wall extract (CAWE, 4 mg/body/day) was administered intraperitoneally to 4-week-old C57BL/6 male mice for 5 consecutive days every 4 weeks for 2 cycles. The mice were euthanized at 4, 8 or 12 weeks after the second administration of CAWE. B: To examine the role of JNK during development of CAWE-induced lesions, the mice were treated with SP600125 (30 mg/kg/day), pharmacological inhibitor of JNK, or placebo for the entire period of the experiment. The mice were euthanized at 4 weeks after the second administration of CAWE.

accompanied with fibrotic thickening of vessel walls. Most of the lesions were fusiform. These macroscopic observations suggested that these might be aneurysmal lesions. We did not find
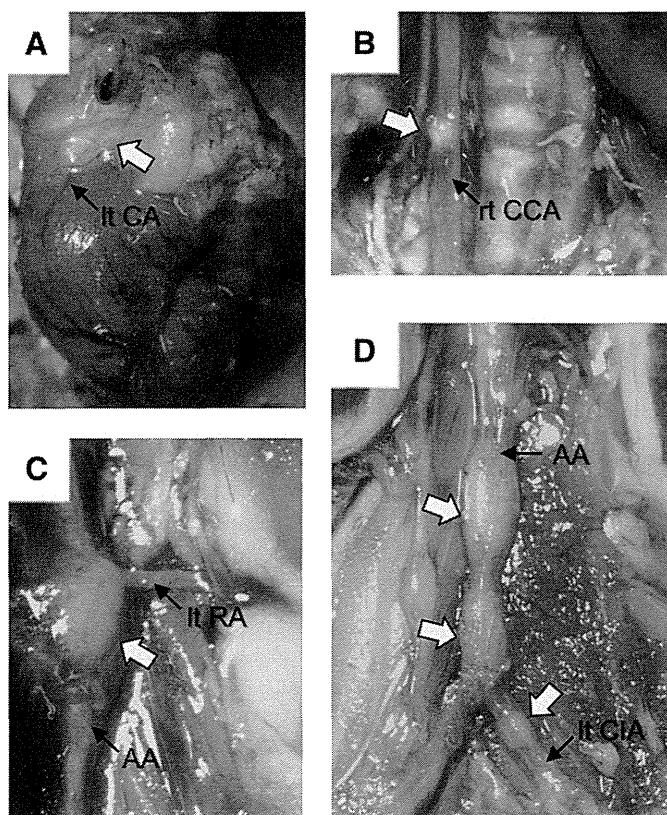

Fig. 2. Development of arterial and aortic lesions induced by CAWE. Representative photographs show the arterial and aortic lesions induced by *Candida albicans* wall extract (CAWE) in mice, as indicated by yellow arrows. A: Lesion of the left coronary artery (lt CA), which was visualized by India ink perfusion. B: Lesion of the right common carotid artery (rt CCA). C: Lesion of the pararenal abdominal aorta (AA) at the level of the left renal artery (lt RA). D: Lesions of the infrarenal abdominal aorta and the left common iliac artery (lt CIA).

thrombotic occlusion or rupture of aneurysm during the experimental period.

Coronary artery lesions were observed near the orifice of the left main coronary artery only in some CAWE-treated mice (Fig. 3A–C). Coronary arteries of untreated control mice showed preserved elastic lamellae, α-SMA$^+$ medial smooth muscle cells, and few inflammatory cells. In contrast, dilated coronary arteries of CAWE-treated mice showed marked inflammatory cell infiltration into all arterial wall layers, straightening and fragmentation of elastic lamellae, disappearance of α-SMA$^+$ cells in the media, and intimal thickening (Fig. 3B and C). Fibrinoid necrosis was not seen in the experimental mice. These findings are similar to pathological features of KD vascular lesions [26]. We also found TN-C to be greatly expressed, associated with cellular infiltration, medial destruction and intimal hyperplasia in the involved arterial walls of CAWE-treated mice (Fig. 3B and C). TN-C is known to be highly upregulated in the vascular system during inflammatory responses, and its expression could be a marker for active tissue remodeling [24].

3.2. Temporal pattern of development of CAWE-induced lesions

We next investigated whether the temporal pattern of pathological processes in CAWE-treated artery accords with that in KD. The incidences of coronary artery lesions were 0.0% (0/7 mice), 14.3% (1/7 mice) and 14.3% (1/7 mice) at 4, 8 and 12 weeks, respectively, after CAWE treatment. In the medium-sized vessels, the incidences of arterial lesions (iliac, coronary, carotid and celiac lesions) were 0.0% (0/7 mice), 42.9% (3/7 mice) and 57.1% (4/7 mice) at 4, 8 and 12 weeks, respectively, after the CAWE treatment (Fig. 4A). Thus, the incidences of lesions in medium vessels were modestly high at 8 and 12 weeks after CAWE treatment, but the incidence of coronary artery lesions was not enough for temporal analysis. Fortunately, the incidences of abdominal aortic lesions were 42.9% (3/7 mice), 57.1% (4/7 mice) and 85.7% (6/7 mice) at 4, 8 and 12 weeks, respectively, after CAWE treatment (Fig. 4A). By the definitions adopted by the 2012 International Chapel Hill Consensus Conference on the Nomenclature of Vasculitides (CHCC2012), KD is classified as part of medium vessel vasculitis (MVV). However, as the CHCC2012 definitions also note that aorta and large arteries may be affected [27,28], we used abdominal aortic lesions in the CAWE-treated mice for further studies.
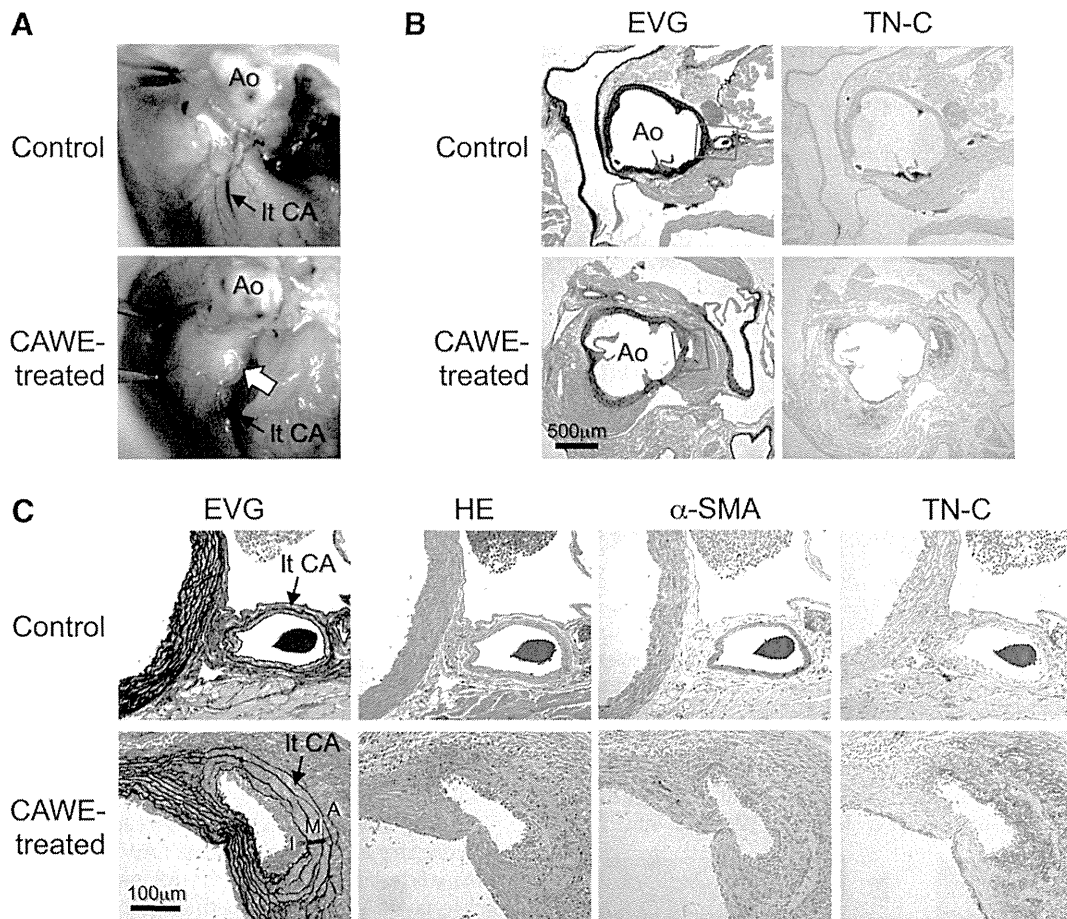
Fig. 3. Development of coronary artery lesions induced by CAWE. A: Representative photographs show the left coronary artery (lt CA) originating from the aorta (Ao) in untreated mice (Control) and mice treated with *Candida albicans* wall extract (CAWE-treated). The left coronary artery was visualized by India ink perfusion. Yellow arrows indicate the coronary artery lesion induced by CAWE. B: Representative histological and immunohistochemical stains are shown for the aorta (Ao) and the left coronary artery of the control and the CAWE-treated mice. C: Representative histological and immunohistochemical stains are shown for enlarged images of the areas within the red squares in the panel B. Elastica van-Gieson (EVG) stain depicts elastin network (black), collagen fibers (red), and muscles (yellow). Hematoxylin/eosin (HE) stain depicts cell nuclei (blue–black). Levels of protein expression and localization of tenascin-C (TN-C) and α-smooth muscle actin (α-SMA) are indicated by brown staining. I: intima, M: media, A: adventitia.

Histological sections of abdominal aortic lesions in CAWE-treated mice also showed similar changes to those of the coronary artery lesions (Fig. 4B and C). At 4 weeks after the CAWE treatment, we observed >marked infiltration of inflammatory cells, including dominant macrophages and lymphocytes, into all layers of the aortic walls. Especially, accumulation of inflammatory cells associated with increased collagen fibers resulted in extensive thickening of the adventitia around the aorta. Although thickness of media and multilayered α-SMA$^+$ smooth muscle cells appeared to be sustained, elastic lamellae began to show straightening and fragmentation. TN-C was widely expressed from intima to adventitia. Inflammatory cell infiltration continued until 8 weeks and gradually decreased at 12 weeks. Destruction of elastic lamellae and thinning of the media progressed until 12 weeks. The α-SMA$^+$ smooth muscle cells completely disappeared in media by 8–12 weeks, whereas neointima consisting of numerous α-SMA$^+$ cells was formed and thickened, leading to stenosis at 12 weeks. TN-C staining was still intense at 8 and 12 weeks, but localized in the thickened intima and the residual media (Fig. 4B and C).

To ascertain if JNK is activated in vascular cells during the development of CAWE-induced lesions, we also examined the tissue localization of p-JNK. Aortic walls of untreated control mice showed few JNK-activated cells. In contrast, dramatic activation of JNK was observed throughout all layers of aortic walls at 4 weeks after CAWE treatment. JNK activation was mostly detected in α-SMA$^+$ smooth muscle cells in the media and the thickened neointima and macrophages were noted in all layers of aortic lesions (Fig. 5A and B).

3.3. Preventive effect of JNK inhibition on development of CAWE-induced lesions

We next investigated whether JNK activation is necessary for development of CAWE-induced lesions. To this end, we subcutaneously implanted the pellets, which were designed to release JNK-specific inhibitor SP600125 (30 mg/kg/day) over the experimental period, in CAWE-treated mice (SP600125 group, n=10). Placebo pellets were also used in CAWE-treated mice as controls (placebo group, n=20). Morphometric analyses of the aortas after perfusion fixation showed that 13 (65.0%) of 20 mice developed abdominal aortic lesions, which reached a certain size and were occasionally accompanied by a "string of beads" appearance, in the placebo group. In contrast, in the SP600125 group, only one (10.0%) of 10 mice developed a small-sized lesion (Fig. 6A and B). Thus, treatment with SP600125 dramatically decreased the incidence of aortic lesions induced by CAWE ($P<0.01$ compared with the placebo group; Fig. 6B), and also significantly reduced the maximum external diameter of the abdominal aorta ($P<0.01$ compared with the placebo group; Fig. 6C). Histological analyses showed that development of lesions was accompanied by marked cellular infiltration into all layers of the aortic wall, extensive destruction of the elastic lamellae in the media, and some intimal thickening in the placebo group. Significant macrophage infiltration and TN-C expression were also extended across all layers of the wall. In sharp contrast, most mice in the SP600125 group showed a few inflammatory cells and preserved elastic lamellae (Fig. 6D). These results indicate that treatment with SP600125 protects
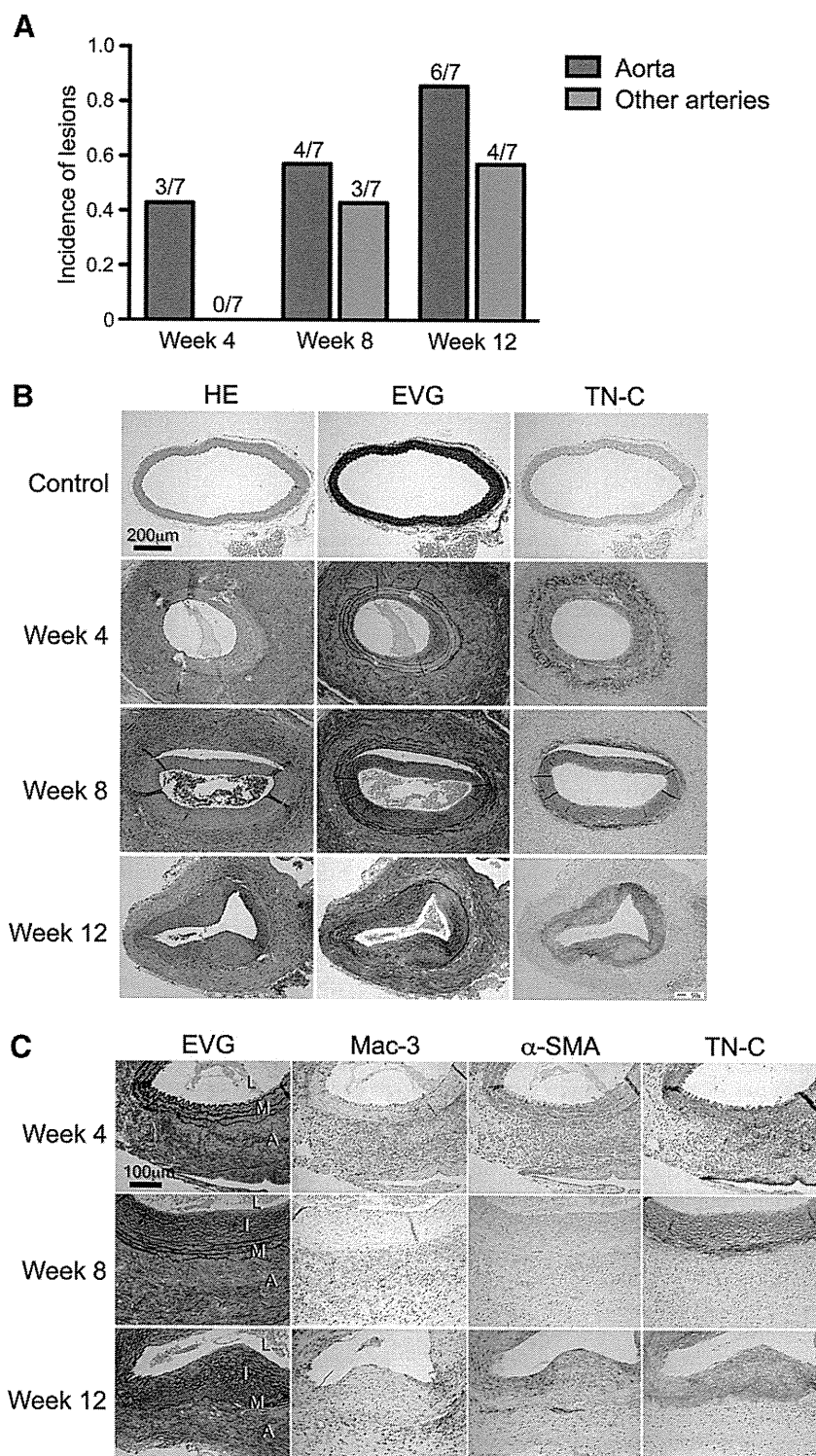
Fig. 4. Development of aortic lesions induced by CAWE. A: Mice treated with *Candida albicans* wall extract (CAWE) developed aortic and arterial lesions. Incidences of aortic and other arterial lesions are shown at 4, 8 or 12 weeks after administration of CAWE. B: Representative histological and immunohistochemical stains are shown for control aorta from untreated control mice and aortic lesions from the mice sacrificed at 4, 8 or 12 weeks after CAWE treatment. C: Representative histological and immunohistochemical stains are shown for enlarged images of aortic lesions from the CAWE-treated mice. Hematoxylin/eosin (HE) stain depicts cell nuclei (blue–black). Elastica van-Gieson (EVG) stain depicts elastin network (black), collagen fibers (red), and muscles (yellow). Levels of protein expression and localization of tenascin-C (TN-C), α-smooth muscle actin (α-SMA) and Mac-3, a macrophage surface glyco-protein, are indicated by brown staining. L: lumen, I: intima, M: media, A: adventitia.

against CAWE-induced vascular inflammation and tissue destruction, resulting in suppressed development of lesions. More interestingly, we also observed TN-C to be significantly expressed only in the medial layer, which appeared undamaged, in the SP600125 group.

This finding indicates that medial smooth muscle cells were not completely normal in the SP600125 group, and might be under certain pathological conditions (convalescence, e.g.) at least 4 weeks after CAWE treatment.
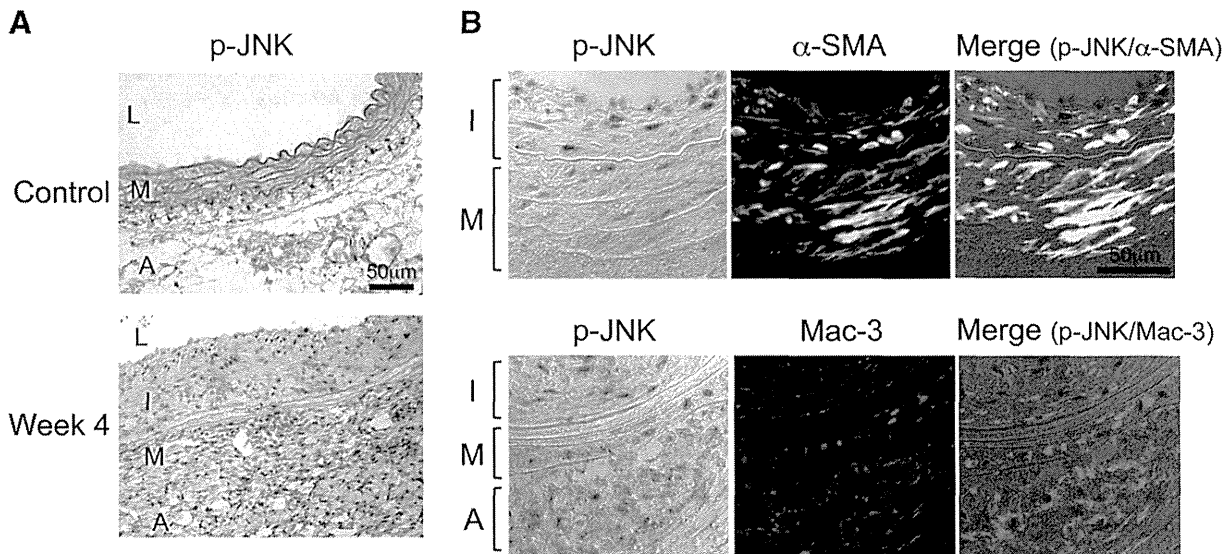
Fig. 5. JNK activation in aortic lesions induced by CAWE. A: Representative immunohistochemical stains are shown for control aorta from untreated control mice and aortic lesions from the mice sacrificed at 4 weeks after CAWE treatment. Localization of phosphorylated JNK (p-JNK) is indicated by brown staining. B: Representative immunohistochemical and immunofluorescence stains are shown for aortic lesions after CAWE treatment. Activated JNK (p-JNK) is indicated by brown staining in differential interference contrast (DIC) images. Localization of α-smooth muscle actin (α-SMA) positive cells or Mac-3 positive macrophages is indicated by green and red fluorescent signals, respectively. L: lumen, I: intima, M: media, A: adventitia.

4. Discussion

The present study clearly showed that pharmacologic inhibition of JNK significantly prevented the development of CAWE-induced vascular lesions in mice. Prior to this demonstration, we administered CAWE to young mice and created the model system, which substantially imitated KD-caused human artery lesions and allowed us to evaluate both macroscopical and histopathological changes in medium-sized arteries and the aorta. Previous imaging studies in patients with KD have shown that coronary artery aneurysms are commonly fusiform or spherical in shape and occasionally form multiple or complex aneurysms, which may show a "string of beads" appearance [3,29–31]. In this study, these macroscopic characteristics were largely recapitulated in both arterial and aortic lesions of our mouse model. Histological studies of autopsy cases with KD-caused coronary artery aneurysms have shown inflammatory cell in filtration into all arterial wall layers, elastic lamellae destruction and intimal thickening [26,29]. In most settings, the medial layer is very thin, whereas the adventitia is thickened by fibrous proliferation [32]. Additionally, fibrinoid necrosis is a characteristic of polyarteritis nodosa, but not KD [27,33]. Our data clearly showed that these hallmark features of KD pathology were fully recapitulated in our CAWE-induced model.

Pathologic changes over time in KD-caused human coronary arterial lesions have been studied previously. Takahashi et al. reported that inflammatory cells infiltrate arterial walls and lead to panvasculitis approximately 10 days after onset of KD [26]. As inflammation progresses, elastic lamellae and smooth muscle cells become severely damaged, eventually resulting in aneurysm formation. Cellular infiltration persists until about 4 weeks after KD onset, after which the acute inflammatory stage gradually transitions into the convalescent stage. Thereafter, in most patients, coronary arteries tend to develop full circumferential intimal thickening, which can cause thrombotic occlusion [2,26]. These temporal aspects of KD arterial lesions were largely reproduced in our CAWE-induced model.

Obviously, our model and human KD differ in some respects. Particularly the highest incidence of vascular lesion is found in coronary arteries in humans [26,27], whereas incidence of aortic lesions was higher than that of coronary artery lesions in our model. However, the size of children's coronary arteries roughly corresponds to that of mouse aorta rather than mouse coronary artery. Therefore, mouse aorta may mimic human coronary artery in the hemodynamic

environment, which potentially affects aneurysm progression [13,34]. In addition, human KD can cause thrombotic occlusion or rupture (a rare complication) in arterial aneurysms [4,26], although neither was observed in this study, probably because of limited period of observation as well as limited number of animals.

KD is linked to various pathogenic agents, including many bacteria and viruses [35]. Many epidemiological findings have pointed out that KD seems like an infectious disease [35,36]. Although the pathogen that triggers human KD has not yet been identified, previous studies, as well as our current study, provide evidence that some bacteria-derived components, such as CAWE and LCWE, can trigger initial systemic inflammation and subsequent local vascular inflammation [8–11,15]. Probably, the systemic inflammation is initiated by recognition of pathogen-associated molecular patterns (PAMPs), which are displayed by CAWE and LCWE; inflammation is then mediated by release of type I interferons and inflammatory cytokines such as tumor necrosis factor (TNF) and interleukin-1 (IL-1) [37,38]. Detection of PAMPs also activates pathogen-specific T and B cells that enhance the inflammatory response, or potentially leads to activation of T and B cells specific for antigens that cross-react with self-antigens [38]. In Candida albicans infection or CAWE administration, recognition of Candida albicans-associated PAMPs through interaction with pattern recognition receptors (PRRs) such as Toll-like receptors and C-type lectin receptors including dectin-1 and dectin-2, initiates production of cytokines and differentiation of T helper-1 (Th1) and Th17 cells [39–41]. These early immune responses are known to involve activation of mitogen-activated protein kinases, including JNK [37,42]. However, based on our observation that TN-C was obviously expressed even in vessel walls of the SP600125-treated mice, we suspect that pharmacologic inhibition of JNK protects against vascular inflammation and lesion formation rather than against the initial immune responses to CAWE.

The mechanism by which initial systemic immune responses to PAMPs lead to the subsequent vascular inflammation is not well understood. Superantigens derived from bacteria and viruses may be involved in this process [15,43,44]. In addition, molecular mimicry that occurs through cross-reactive recognition between a microbial antigen/MHC and a self-antigen/MHC complex could be also responsible for this onset of vasculitis [38]. In the initiation of vasculitis, as proposed previously, inflammatory cells such as macrophages, neutrophils and T cells are recruited to the vascular walls, and various cytokines/chemokines are released. Coincidentally, endothelial cells and vascular smooth
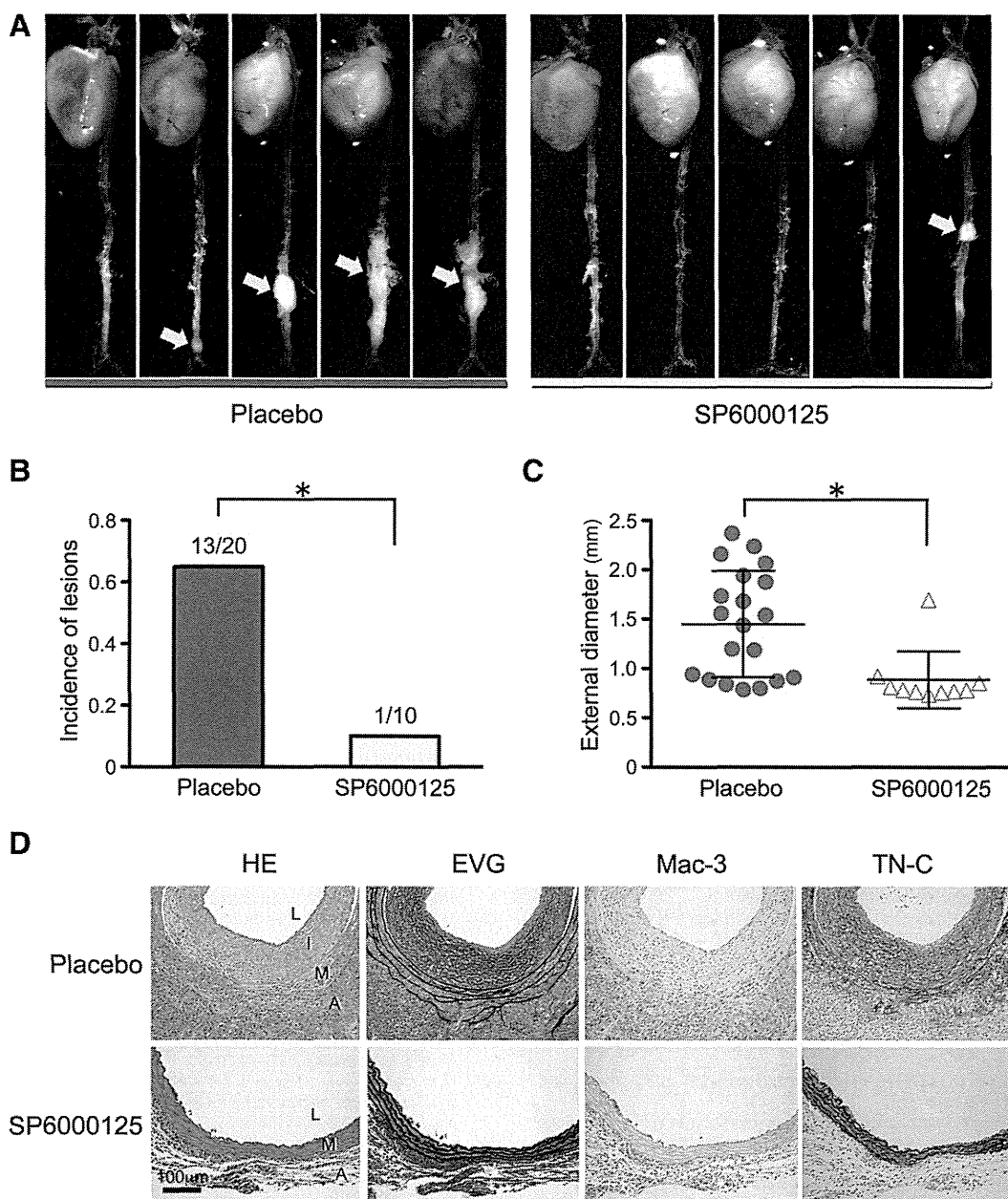
Fig. 6. Effect of JNK inhibition on development of CAWE-induced lesions. **A:** Representative photographs show the aortas of the mice treated with SP600125, JNK inhibitor, or placebo at 4 weeks after administration of *Candida albicans* wall extract (CAWE). **B:** Incidences of aortic lesions induced by CAWE are shown for the mice treated with SP600125 or placebo. **C:** Maximum external diameters of abdominal aortas are shown for the CAWE-treated mice with SP600125 or placebo. Data are mean±SD. * P<0.01 compared to placebo. **D:** Representative histological and immunohistochemical stains are shown for the abdominal aortas of the CAWE-treated mice with SP600125 or placebo. Hematoxylin/eosin (HE) stain depicts cell nuclei (blue–black). Elastica van-Gieson (EVG) stain depicts elastin network (black), collagen fibers (red), and muscles (yellow). Levels of protein expression and localization of tenascin-C (TN-C) and Mac-3 are indicated by brown staining. L: lumen, I: intima, M: media, A: adventitia.

muscle cells are also stimulated to produce cytokines/chemokines, which augment inflammatory cell accumulation [15,40]. During these events, JNK can be activated by stimulation with proinflammatory cytokines such as TNF and IL-1 in various cells, including vascular smooth muscle cells and macrophages [23,37]. Activation of JNK also upregulates the genes that encode proinflammatory cytokines such as TNF and IL-1 [21,45,46], thus enhancing these inflammatory responses. A role for JNK in prolongation of vascular inflammation has also been suggested [34,47]. Persistent activation of JNK then contributes to prolonged chronic inflammation and eventually shifts the balance of extracellular matrix metabolism toward degradation by upregulating MMP activity, thereby leading to development of aneurysmal lesions [22,23]. In addition, JNK may also enhance lesion formation by reducing extracellular matrix biosynthetic enzymes including lysyl oxydase [45]

and by mediating apoptosis of vascular smooth muscle cells [48]. Moreover, JNK is reportedly involved in intimal thickening [49], which is typically accompanied by KD-related lesions. Taken together, these data suggest that JNK activation accelerates not only vasculitis but also KD-caused aneurysmal lesions, through multiple mechanisms. We have demonstrated, in fact, that inhibiting JNK suppresses inflammatory cell infiltration, destruction of elastic lamellae and intimal thickening, resulting in effective prevention of lesion formation in our CAWE-induced model.

In conclusion, this study has shown, for the first time, that JNK activation is critical to development of CAWE-induced vascular lesions in mice, and provided novel insights into the role of JNK in the pathogenesis of KD-caused lesion formation. Although further studies are needed to determine the efficacy and safety of JNK inhibition in

KD, our findings suggest that JNK could be a novel therapeutic target in patients with vascular lesions and those at high risk for aneurysms due to nonresponsiveness to current standard therapy.

Acknowledgments

The authors thank M. Namikata for providing technical assistance.

References

[1] Kawasaki T, Kosaki F, Okawa S, Shigematsu I, Yanagawa H. A new infantile acute febrile mucocutaneous lymph node syndrome (MLNS) prevailing in Japan. Pediatrics 1974;54:271–6.
[2] Burns JC, Glode MP. Kawasaki syndrome. Lancet 2004;364:533–44.
[3] Newburger JW, Takahashi M, Gerber MA, Gewitz MH, Tani LY, Burns JC, et al. Diagnosis, treatment, and long-term management of Kawasaki disease: a statement for health professionals from the Committee on Rheumatic Fever, Endocarditis and Kawasaki Disease, Council on Cardiovascular Disease in the Young, American Heart Association. Circulation 2004;110:2747–71.
[4] Senzaki H. Long-term outcome of Kawasaki disease. Circulation 2008;118:2763–72.
[5] Furusho K, Kamiya T, Nakano H, Kiyosawa N, Shinomiya K, Hayashidera T, et al. High-dose intravenous gammaglobulin for Kawasaki disease. Lancet 1984;2:1055–8.
[6] Gordon JB, Kahn AM, Burns JC. When children with Kawasaki disease grow up: myocardial and vascular complications in adulthood. J Am Coll Cardiol 2009;54:1911–20.
[7] Daniels LB, Tjajadi MS, Walford HH, Jimenez-Fernandez S, Trofimenko V, Fick DB, et al. Prevalence of Kawasaki disease in young adults with suspected myocardial ischemia. Circulation 2012;125:2447–53.
[8] Lehman TJ, Walker SM, Mahnovski V, McCurdy D. Coronary arteritis in mice following the systemic injection of group B Lactobacillus casei cell walls in aqueous suspension. Arthritis Rheum 1985;28:652–9.
[9] Takahashi K, Oharaseki T, Wakayama M, Yokouchi Y, Naoe S, Murata H. Histopathological features of murine systemic vasculitis caused by Candida albicans extract—an animal model of Kawasaki disease. Inflamm Res 2004;53:72–7.
[10] Lee Y, Schulte DJ, Shimada K, Chen S, Crother TR, Chiba N, et al. Interleukin-1beta is crucial for the induction of coronary artery inflammation in a mouse model of Kawasaki disease. Circulation 2012;125:1542–50.
[11] Oharaseki T, Yokouchi Y, Yamada H, Mamada H, Muto S, Sadamoto K, et al. The role of TNF-alpha in a murine model of Kawasaki disease arteritis induced with a Candida albicans cell wall polysaccharide. Mod Rheumatol 2013.
[12] Martinez HG, Quinones MP, Jimenez F, Estrada C, Clark KM, Suzuki K, et al. Important role of CCR2 in a murine model of coronary vasculitis. BMC Immunol 2012;13:56.
[13] Tedesco MM, Dalman RL. Arterial aneurysms. In: Cronenwett JL, Johnston KW, editors. Vascular surgery. Philadelphia: Saunders; 2010. p. 117–30.
[14] Yoshimura K, Aoki H. Recent advances in pharmacotherapy development for abdominal aortic aneurysm. Int J Vasc Med 2012;2012:648167.
[15] Yeung RS. Kawasaki disease: update on pathogenesis. Curr Opin Rheumatol 2010;22:551–60.
[16] Chalouhi N, Hoh BL, Hasan D. Review of cerebral aneurysm formation, growth, and rupture. Stroke 2013;44:3613–22.
[17] Nagasawa A, Yoshimura K, Suzuki R, Mikamo A, Yamashita O, Ikeda Y, et al. Important role of the angiotensin II pathway in producing matrix metalloproteinase-9 in human thoracic aortic aneurysms. J Surg Res 2013.
[18] Aoki T, Kataoka H, Morimoto M, Nozaki K, Hashimoto N. Macrophage-derived matrix metalloproteinase-2 and -9 promote the progression of cerebral aneurysms in rats. Stroke 2007;38:162–9.
[19] Lau AC, Duong TT, Ito S, Yeung RS. Matrix metalloproteinase 9 activity leads to elastin breakdown in an animal model of Kawasaki disease. Arthritis Rheum 2008;58:854–63.
[20] Gavin PJ, Crawford SE, Shulman ST, Garcia FL, Rowley AH. Systemic arterial expression of matrix metalloproteinases 2 and 9 in acute Kawasaki disease. Arterioscler Thromb Vasc Biol 2003;23:576–81.
[21] Zhang YL, Dong C. MAP kinases in immune responses. Cell Mol Immunol 2005;2:20–7.
[22] Yoshimura K, Aoki H, Ikeda Y, Furutani A, Hamano K, Matsuzaki M. Identification of c-Jun N-terminal kinase as a therapeutic target for abdominal aortic aneurysm. Ann N Y Acad Sci 2006;1085:403–6.
[23] Yoshimura K, Aoki H, Ikeda Y, Fujii K, Akiyama N, Furutani A, et al. Regression of abdominal aortic aneurysm by inhibition of c-Jun N-terminal kinase. Nat Med 2005;11:1330–8.
[24] Kimura T, Yoshimura K, Aoki H, Imanaka-Yoshida K, Yoshida T, Ikeda Y, et al. Tenascin-C is expressed in abdominal aortic aneurysm tissue with an active degradation process. Pathol Int 2011;61:559–64.
[25] Imanaka-Yoshida K, Hiroe M, Nishikawa T, Ishiyama S, Shimojo T, Ohta Y, et al. Tenascin-C modulates adhesion of cardiomyocytes to extracellular matrix during tissue remodeling after myocardial infarction. Lab Invest 2001;81:1015–24.
[26] Takahashi K, Oharaseki T, Yokouchi Y, Naoe S, Saji T. Kawasaki disease: basic and pathological findings. Clin Exp Nephrol 2013;17:690–3.
[27] Jennette JC, Falk RJ, Bacon PA, Basu N, Cid MC, Ferrario F, et al. 2012 revised International Chapel Hill Consensus Conference nomenclature of vasculitides. Arthritis Rheum 2013;65:1–11.
[28] Jennette JC. Overview of the 2012 revised International Chapel Hill Consensus Conference nomenclature of vasculitides. Clin Exp Nephrol 2013;17:603–6.
[29] Naoe S, Takahashi K, Masuda H, Tanaka N. Kawasaki disease. With particular emphasis on arterial lesions. Acta Pathol Jpn 1991;41:785–97.
[30] Goo HW, Park IS, Ko JK, Kim YH. Coronary CT angiography and MR angiography of Kawasaki disease. Pediatr Radiol 2006;36:697–705.
[31] Baker AL, Newburger JW. Cardiology patient pages. Kawasaki disease. Circulation 2008;118:e110–2.
[32] Suzuki A, Miyagawa-Tomita S, Komatsu K, Nishikawa T, Sakomura Y, Horie T, et al. Active remodeling of the coronary arterial lesions in the late phase of Kawasaki disease: immunohistochemical study. Circulation 2000;101:2935–41.
[33] Takahashi K, Oharaseki T, Yokouchi Y. Pathogenesis of Kawasaki disease. Clin Exp Immunol 2011;164(Suppl 1):20–2.
[34] Yamashita O, Yoshimura K, Nagasawa A, Ueda K, Morikage N, Ikeda Y, et al. Periostin links mechanical strain to inflammation in abdominal aortic aneurysm. PLoS One 2013;8:e79753.
[35] Principi N, Rigante D, Esposito S. The role of infection in Kawasaki syndrome. J Infect 2013;67:1–10.
[36] Frazer J. Infectious disease: blowing in the wind. Nature 2012;484:21–3.
[37] Gaestel M, Kotlyarov A, Kracht M. Targeting innate immunity protein kinase signalling in inflammation. Nat Rev Drug Discov 2009;8:480–99.
[38] Munz C, Lunemann JD, Getts MT, Miller SD. Antiviral immune responses: triggers of or triggered by autoimmunity? Nat Rev Immunol 2009;9:246–58.
[39] Cassone A. Development of vaccines for Candida albicans: fighting a skilled transformer. Nat Rev Microbiol 2013;11:884–91.
[40] Takahashi K, Oharaseki T, Yokouchi Y. Update on etio and immunopathogenesis of Kawasaki disease. Curr Opin Rheumatol 2014;26:31–6.
[41] Lin IC, Suen JL, Huang SK, Huang SC, Huang HC, Kuo HC, et al. Dectin-1/Syk signaling is involved in Lactobacillus casei cell wall extract-induced mouse model of Kawasaki disease. Immunobiology 2013;218:201–12.
[42] Arthur JS, Ley SC. Mitogen-activated protein kinases in innate immunity. Nat Rev Immunol 2013;13:679–92.
[43] Devore-Carter D, Kar S, Vellucci V, Bhattacherjee V, Domanski P, Hostetter MK. Superantigen-like effects of a Candida albicans polypeptide. J Infect Dis 2008;197:981–9.
[44] Duong TT, Silverman ED, Bissessar MV, Yeung RS. Superantigenic activity is responsible for induction of coronary arteritis in mice: an animal model of Kawasaki disease. Int Immunol 2003;15:79–89.
[45] Yoshimura K, Aoki H, Ikeda Y, Furutani A, Hamano K, Matsuzaki M. Regression of abdominal aortic aneurysm by inhibition of c-Jun N-terminal kinase in mice. Ann N Y Acad Sci 2006;1085:74–81.
[46] Guma M, Firestein GS. c-Jun N-terminal kinase in inflammation and rheumatic diseases. Open Rheumatol J 2012;6:220–31.
[47] Onoda M, Yoshimura K, Aoki H, Ikeda Y, Morikage N, Furutani A, et al. Lysyl oxidase resolves inflammation by reducing monocyte chemoattractant protein-1 in abdominal aortic aneurysm. Atherosclerosis 2010;208:366–9.
[48] Takagi Y, Ishikawa M, Nozaki K, Yoshimura S, Hashimoto N. Increased expression of phosphorylated c-Jun amino-terminal kinase and phosphorylated c-Jun in human cerebral aneurysms: role of the c-Jun amino-terminal kinase/c-Jun pathway in apoptosis of vascular walls. Neurosurgery 2002;51:997–1002 [discussion—4].
[49] Izumi Y, Kim S, Namba M, Yasumoto H, Miyazaki H, Hoshiga M, et al. Gene transfer of dominant-negative mutants of extracellular signal-regulated kinase and c-Jun NH2-terminal kinase prevents neointimal formation in balloon-injured rat artery. Circ Res 2001;88:1120–6.

Molecular Genetics & Genomic Medicine

LETTER TO THE EDITOR

Kawasaki disease patients homozygous for the rs12252-C variant of interferon-induced transmembrane protein-3 are significantly more likely to develop coronary artery lesions

Kawasaki disease (KD) is the most common systemic vasculitis syndrome, primarily affecting small- to medium-sized arteries, more particularly the coronary arteries (Kato et al. 1996). KD was first described in 1967 and is now identified as the leading cause of acquired heart disease among children in developed countries (Wang et al. 2005). The annual incidence of KD in children of Japanese descent is about 218 per 100,000 children less than 5 years of age (Nakamura et al. 2012) as compared to about 20 per 100,000 in the United States (Holman et al. 2010a). Timely treatment with high-dose intravenous γ globulin (IVIG) reduces the duration of fever and incidence of coronary artery lesions (CAL). However, even after IVIG treatment ~5–7% of patients develop aneurysms (Ogata et al. 2013).

It is widely believed that KD is induced by one or more infectious agents that evoke an abnormal immunological response in genetically susceptible individuals (Burgner and Harnden 2005). However, since the initial description of KD, identification of a definitive infectious agent has been elusive. Several lines of evidence support the infection hypothesis including the acute onset of a self-limited illness, increased susceptibility at younger age, and geographic clustering of outbreaks with a seasonal predominance (later winter and early spring) (Wang et al. 2005).

There is a higher incidence of KD in Japan as well as among Japanese descendants residing in the United States than in any other ethnic populations (Holman et al. 2010b), suggesting that a genetic predisposition also plays an important role in susceptibility to the disease. In addition, there is evidence that the incidence of KD in parents and siblings of an affected patient is higher than in the general population (Onouchi 2012). For example, it has been reported that siblings of affected children are at 10- to 30-fold greater risk of developing KD than children in the general population (Fujita et al. 1989). In addition, offspring of individuals diagnosed with KD are more likely to develop KD (Uehara et al. 2004). More recently there have been a large number of genetic linkage and genome-wide association studies (GWAS) that have reported genetic loci associated with risk and outcomes, see Onouchi (2012) for a comprehensive review. Among the loci that have been implicated in large GWAS studies and have been replicated by separate studies are FCGR2A (Khor et al. 2011; Onouchi et al. 2012), CASP3 (Onouchi et al. 2010; Kuo et al. 2013), and BLK (Onouchi et al. 2012; Chang et al. 2013).

HLA-B haplotypes have also been linked to KD with one study identifying KD-associated polymorphisms in ABHD16A (abhydrolase domain containing 16A; also known as BAT5: HLA-B associated transcript 5) (Hsieh et al. 2010), this association has not been replicated by other studies. ABHD16A encodes a highly conserved, widely expressed lipase of unknown specificity although it has been proposed to function as a palmitoylthioesterase (Martin et al. 2012). ABHD16A binds to IFITM1 (interferon-induced transmembrane protein 1) (Lehner et al. 2004). Another member of the family, IFITM3 (OMIM: 605579), is transcriptionally induced by type I and II interferons and serves to block cellular infection by viruses (such as influenza and dengue) that require endosomal entry into the cytoplasm for replication (Brass et al. 2009; Jiang et al. 2010; Weidner et al. 2010; Lu et al. 2011).

An allelic variant in the human IFITM3 gene (SNP rs12252: NM_021034.2:c.42T>C; p.Ser14=) truncates the first 20 amino acids of the protein by introducing an alternative splice site and results in the loss of its "antiviral" function (Everitt et al. 2012). Everitt and colleagues also showed that for European Caucasian patients infected with influenza A H1N1/09 virus, those homozygous for the C allele were significantly more likely to develop severe infections requiring hospitalization. More recently, Zhang et al. (2013) made a similar observation in Chinese patients infected with H1N1/09 influenza. The objectives of the study were (1) to evaluate for differences in IFITM3 genotype frequencies between KD and control cohorts, (2) to assess whether there are differences in the incidences of CAL among the three KD genotypes, and (3) to assess for differences in the distributions of demographic factors (age, gender), IVIG treatment, laboratory data (C-reactive protein [CRP] levels and numbers of white blood cells [WBC]), and duration of fever.

In this study, we genotyped 140 KD patients recruited at three centers, the University of Toyama ($n = 89$),

Kanazawa Medical University ($n = 10$), and the University of Utah ($n = 41$), for the rs12252 SNP. Patients were diagnosed with KD according to standard diagnostic criteria (Kawasaki et al. 1974; Kawasaki 1979). All patients were treated with IVIG and oral aspirin at the time of diagnosis. Echocardiography was used to determine whether the patients had developed CAL, defined as a coronary artery with a diameter of 3 mm or more (4 mm if the subject was over the age of 5 year) at ≥1 month after the onset of KD (Shulman et al. 1995).

With informed consent, venous blood samples or buccal swabs were obtained at the time of diagnosis and DNA isolated and stored at −20°C. For genotyping, both coding exons of *IFITM3* were amplified from 10 ng of genomic DNA using Platinum *Taq* polymerase (Life Technologies, Carlsbad, CA) (Arrington et al. 2012) and the oligonucleotide primers, IFITM3_1_F: 5′-CAAATGCCAGGAAAAGGA AA-3′ and IFITM3_2_R: 5′-CGAGGAATGGAAGTTGGA GT-3′. The 1158 bp PCR product was analyzed by agarose gel electrophoresis, purified by treating with Exo-SAP-IT (Affymetrix, Santa Clara, CA), and then submitted to the University of Utah DNA sequencing core for analysis (Arrington et al. 2012). The study was approved by the Ethics Committees of the University of Toyama and the Kanazawa Medical University, and the Institutional Review Board of the University of Utah.

Corresponding to the three objectives stated above, we carried out the analyses and summarized the results in three tables. In the first analysis (Table 1), we reported the distribution of KD allele and genotype frequency for the control and the KD (case) cohort. The percentage was the conditional probability of having the specific allele or genotype category. These conditional probabilities were compared between the control and case cohort, stratified by race (white, Japanese), by using the chi-square test, or the Fisher's Exact test when the frequency count was less than 5 in at least one cell in the contingency table. In the second analysis (Table 2), the association between CAL incidence and genotype was assessed using either

chi-square test or Fisher's exact test. We performed four different contingency table analyses for the overall KD cohort (genotype, allele, dominant, recessive) and thus have used an adjusted type-I error by the Bonferroni method (by dividing the level of significance 0.05 by 4 which yield 0.0125). Thus, the *P*-value was considered significant if it was less than 0.0125 instead of 0.05. Similarly, we performed this analysis for the stratified cohort of Asian, and white patients. In the third analysis (Table 3), we first assessed the shape of the distribution of the continuous variable of age, CRP, WBC, and fever duration and learned using the normality test of Shapiro–Wilk and examined the histograms that these variables did not follow near normal distribution. Thus, we also reported the median in addition to the mean and standard deviation, overall, and for each of the three genotype categories. We used the nonparametric Wilcoxon rank-sum test to compare among the three groups of genotype. For gender, and treatment response to IVIG, we used either chi-square or Fisher's exact test. For this table, since all the comparisons were preplanned, and no pair-wise comparisons were done, we maintained the type-I error at 0.05. All of our analyses were carried out using the SAS/STAT software version 9.3 (Cary, NC) (procedure FREQ for chi-square or Fisher's exact test, and procedure NPAR1WAY for the nonparametric Wilcoxon rank-sum test). Allelic and genotype frequencies were assessed for Hardy–Weinberg equilibrium using the online calculator at http://www.oege.org/software/hwe-mr-calc.shtml (Rodriguez et al. 2009).

All 99 patients recruited in Toyama and Kanazawa were of Japanese descent. Of the 41 patients recruited in Utah, 37 were Caucasian (five with Hispanic ethnicity), 1 Asian, 1 Pacific Islander, and 2 Alaskan Native/Native American. Comparing the allelic frequencies and genotype distribution for rs12252 in the KD Caucasian/non-Hispanic and Japanese patients with 1000 genome (1000g) data from 170 Caucasian/non-Hispanic and 178 Japanese patients who did not have KD (control), did not reveal a

Table 1. Allele and genotype frequencies of the SNP rs12252 (NM_021034.2:c.42T>C) in Utah Caucasian/non-Hispanic and Japanese patients with KD, compared with 1000 genome data for Utah and Japanese controls.

Genotype	Controls (1000g CEU: $n = 170$)	Utah White-non Hispanic cases ($n = 32$)	*P*-value	Controls (1000g JPT: $n = 178$)	Japanese cases ($n = 99$)	*P*-value
Allele C	16 (5%)	5 (8%)	0.352	210 (63%)	121 (65%)	0.625
Allele T	324 (95%)	59 (92%)		146 (37%)	77 (35%)	
CC	0 (0%)	0 (0%)	0.358	68 (38%)	38 (38%)	0.683
CT	16 (9%)	5 (16%)		74 (42%)	45 (46%)	
TT	154 (91%)	27 (84%)		36 (20%)	16 (16%)	

P values were obtained by chi-square test or Fisher's exact test.

357

Table 2. The C allele and CC genotype for rs12252 (NM_021034.2:c.42T>C) are significantly associated with the development of CAL in KD patients.

			Contingency table		P value
All patients					
Genotype		CC	CT	TT	
	CAL	21 (51%)	13 (26%)	10 (20%)	0.004
	No CAL	20 (49%)	37 (74%)	39 (80%)	
Allelic frequency		C	T		
	CAL	55 (42%)	33 (22%)		0.0004
	No CAL	76 (58%)	116 (78%)		
Genetic model					
Dominant		CC + CT	TT		
	CAL	34 (37%)	10 (20%)		0.039
	No CAL	57 (63%)	39 (80%)		
Recessive		CC	CT + TT		
	CAL	21 (51%)	23 (23%)		0.001
	No CAL	20 (49%)	76 (77%)		
Asian patients					
Genotype		CC	CT	TT	
	CAL	20 (51%)	12 (27%)	3 (19%)	0.025
	No CAL	19 (49%)	33 (77%)	13 (81%)	
Allelic frequency		C	T		
	CAL	52 (42%)	18 (23%)		0.006
	No CAL	71 (58%)	59 (77%)		
Genetic model					
Dominant		CC + CT	TT		
	CAL	32 (38%)	3 (19%)		0.164
	No CAL	52 (62%)	13 (81%)		
Recessive		CC	CT + TT		
	CAL	20 (51%)	15 (25%)		0.009
	No CAL	19 (49%)	46 (75%)		
Caucasian patients					
Genotype		CC	CT	TT	
	CAL	0 (0%)	1 (20%)	7 (23%)	1.000
	No CAL	1 (100%)	4 (80%)	24 (77%)	
Allelic frequency		C	T		
	CAL	1 (14%)	15 (22%)		1.000
	No CAL	6 (86%)	52 (78%)		
Genetic model					
Dominant		CC + CT	TT		
	CAL	1 (17%)	7 (23%)		1.000
	No CAL	5 (83%)	24 (77%)		
Recessive		CC	CT + TT		
	CAL	0 (0%)	8 (22%)		1.000
	No CAL	1 (100%)	28 (78%)		

P values were obtained by chi-square analysis.

significant difference in either (Table 1), all genotypes were in Hardy–Weinberg equilibrium. Three patients from Utah were homozygous CC, the Asian and Pacific Islander patients as well as one of the Caucasian/Hispanic patients.

Further analysis of the allelic frequencies and genotype distribution for rs12252 identified a significant association with outcome. Patients who developed CAL were significantly more likely to carry the C allele (*P* = 0.0004) and the distribution of genotypes was significantly different

(*P* = 0.004) (Table 2). In addition, significantly more patients homozygous for the SNP developed CAL than patients with the other genotypes (51.2% vs. 23.2%: *P* = 0.001), supporting a recessive model for the effect of this SNP (Table 2). There was not a significant association with a dominant model (*P* = 0.039). These associations were also true when comparing outcomes in Asian patients (Table 2). There was not a significant association for Caucasians, possibly because the minor allele is very

Table 3. Comparison of clinical and laboratory data in KD patients with different rs12252 (NM_021034.2:c.42T>C) genotypes.

Demographic	All KD (*N* = 140)	CC (*N* = 41)	CT (*N* = 50)	TT (*N* = 49)	*P* value
All patients					
Age at Dx (years)	2.73 ± 2.38 (2.37)	2.63 ± 2.58 (1.80)	2.76 ± 2.16 (2.00)	2.78 ± 2.45 (2.50)	0.718[1]
Gender (M/F)	94/46	29/12	29/21	36/13	0.221[2]
Second dose of IVIG required	31/139[3]	9/40	11/50[3]	11/49	0.968[2]
Laboratory data[4]					
CRP (mg/dL)	10.23 ± 7.61 (8.40)	8.71 ± 7.11 (6.37)	9.99 ± 5.82 (8.55)	11.67 ± 9.24 (8.85)	0.289[1]
WBC/μL	15,103 ± 4974 (14,510)	15,347 ± 5466 (15,570)	14,174 ± 4559 (13,400)	15,752 ± 4922 (14,555)	0.303[1]
Duration of fever (days)	9.35 ± 4.90 (8.00)	10.47 ± 5.72 (8.50)	9.60 ± 4.42 (9.00)	8.27 ± 4.52 (6.00)	0.055[1]
Asian patients	All KD (*N* = 100)	CC (*N* = 39)	CT (*N* = 45)	TT (*N* = 16)	*P* value
Age at Dx (years)	2.62 ± 2.10 (1.90)	2.42 ± 2.07 (1.80)	2.74 ± 2.16 (2.00)	2.72 ± 2.09 (2.70)	0.607[1]
Gender (M/F)	64/36	27/12	26/19	11/5	0.503[2]
Second dose of IVIG required	23/99	8/38	11/45[3]	4/16	0.956[2]
Laboratory data					
CRP (mg/dL)	9.21 ± 6.39 (7.80)	8.28 ± 6.63 (6.37)	9.71 ± 5.84 (8.50)	9.92 ± 7.21 (6.75)	0.303[1]
WBC/μL	14,427 ± 4847 (13,900)	15,047 ± 5459 (15,000)	14,116 ± 4848 (13,500)	13,869 ± 3521 (13,130)	0.566[1]
Duration of fever (days)	10.02 ± 5.22 (9.00)	10.81 ± 5.72 (9.00)	9.69 ± 4.40 (9.00)	9.20 ± 6.05 (6.00)	0.323[1]
Caucasian patients	All KD (*N* = 37)	CC (*N* = 1)	CT (*N* = 5)	TT (*N* = 31)	*P* value
Age at Dx (years)	2.75 ± 2.63 (2.00)	1.1 ± NA (1.1)	2.9 ± 2.44 (2.00)	2.78 ± 2.72 (2.40)	0.853[1]
Gender (M/F)	27/10	1/0	3/2	23/8	0.711[2]
Second dose of IVIG required	7/37	1/0	0/5	6/31	0.455[2]
Laboratory data					
CRP (mg/dL)	12.56 ± 9.74 (12.20)	5.10 ± NA (5.10)	11.86 ± 5.92 (13.50)	13.03 ± 10.56 (12.20)	0.747[1]
WBC/μL	16,443 ± 5010 (15,250)	17,800 ± NA (17,800)	14,560 ± 2152 (13,300)	16,779 ± 5466 (15,250)	0.530[1]
Duration of fever (days)	7.76 ± 3.66 (6.00)	5.00 ± NA (5.00)	9.00 ± 5.05 (6.00)	7.64 ± 3.47 (6.00)	0.43[1]

Mean ± SD and median values (in parentheses) are reported. Dx, diagnosis; SD, standard deviation; M, male; F, female; IVIG, intravenous γ globulin; CRP, C-reactive protein; WBC, white blood cells; μL, microliter; NA, not applicable (one patient).
[1]*P* values obtained by nonparametric Wilcoxon rank-sum test.
[2]*P* values obtained by chi-square test and Fisher's exact test when cell counts <5.
[3]Data for one patient incomplete.
[4]Laboratory data incomplete for 31 of the 140 patients; 9 CC, 12 CT, and 10 TT.

rare in this population limiting the power of the comparison in this small cohort. There were no significant differences in other clinical and laboratory data between genotypes (Table 3), including the duration of fever and the response to IVIG.

The IFITM proteins restrict the cellular entry of various viruses, including influenza A, flaviviruses, dengue virus, West Nile virus, and severe acute respiratory syndrome coronavirus (Brass et al. 2009; Huang et al. 2011). These viruses share common characteristics in that they are enveloped and enter cells via membrane fusion in endosomal compartments. It has been shown that IFITM3 prevents emergence of viral genomes from the endosomal pathway, although this may be restricted to late endosomes or lysosomes (Feeley et al. 2011). Since many enveloped viruses enter host cells through the late endocytic pathway, it is possible that enveloped viruses are an important etiologic agent in KD, particularly in patients that develop CAL. The symptoms of KD suggest that tissue damage may also occur from an over-reaction of the

immune response characterized by the elevated expression of inflammatory cytokines (Saji and Kemmotsu 2006). The IFITM proteins of man and mouse have also been shown to be associated with membrane signaling complexes (Smith et al. 2006), consequently the loss of functional IFITM3 in KD patients may predispose to enhanced inflammatory responses and tissue damage.

Among the Japanese cohort, 19 (50%) of 38 patients carrying the CC genotype developed CAL. In the Utah cohort, 2 (66.7%) of 3 patients homozygous for rs12252-C developed CAL. At least in the Asian population, where the frequency of the C allele is high, screening for this SNP may be a relatively cost effective way to identify patients at higher risk of developing CAL.

In conclusion, our data reveal a novel association between the *IFITM3* rs12252 CC genotype and the development of CAL in patients with KD, particularly in Asian patients. This association did not extend to the susceptibility to develop KD but it is noteworthy that the frequency of this allele is much higher in the Asian

population, as is the frequency of KD. Since this variant leads to production of a truncated protein with reduced ability to block viral release from the endocytic pathway, these data suggest enveloped viruses may be an important etiologic agent for KD and/or the development of CAL.

Acknowledgments

Conflict of Interest

None declared.

References

Arrington, C. B., S. B. Bleyl, N. Matsunami, G. D. Bonnell, B. E. Otterud, D. C. Nielsen, et al. 2012. Exome analysis of a family with pleiotropic congenital heart disease. Circ. Cardiovasc. Genet. 5:175–182.

Brass, A. L., I. C. Huang, Y. Benita, S. P. John, M. N. Krishnan, E. M. Feeley, et al. 2009. The IFITM proteins mediate cellular resistance to influenza A H1N1 virus, West Nile virus, and dengue virus. Cell 139: 1243–1254.

Burgner, D., and A. Harnden. 2005. Kawasaki disease: what is the epidemiology telling us about the etiology? Int. J. Infect. Dis. 9:185–194.

Chang, C. J., H. C. Kuo, J. S. Chang, J. K. Lee, F. J. Tsai, C. C. Khor, et al. 2013. Replication and meta-analysis of GWAS identified susceptibility loci in kawasaki disease confirm the importance of B lymphoid tyrosine kinase (BLK) in disease susceptibility. PLoS One 8:e72037.

Everitt, A. R., S. Clare, T. Pertel, S. P. John, R. S. Wash, S. E. Smith, et al. 2012. IFITM3 restricts the morbidity and mortality associated with influenza. Nature 484:519–523.

Feeley, E. M., J. S. Sims, S. P. John, C. R. Chin, T. Pertel, L. M. Chen, et al. 2011. IFITM3 inhibits influenza A virus infection by preventing cytosolic entry. PLoS Pathog. 7:e1002337.

Fujita, Y., Y. Nakamura, K. Sakata, N. Hara, M. Kobayashi, M. Nagai, et al. 1989. Kawasaki disease in families. Pediatrics 84:666–669.

Holman, R. C., E. D. Belay, K. Y. Christensen, A. M. Folkema, C. A. Steiner, and L. B. Schonberger. 2010a. Hospitalizations for Kawasaki syndrome among children in the United States, 1997–2007. Pediatr. Infect. Dis. J. 29:483–488.

Holman, R. C., K. Y. Christensen, E. D. Belay, C. A. Steiner, P. V. Effler, J. Miyamura, et al. 2010b. Racial/ethnic differences in the incidence of Kawasaki syndrome among children in Hawaii. Hawaii Med. J. 69:194–197.

Hsieh, Y. Y., Y. J. Lin, C. C. Chang, D. Y. Chen, C. M. Hsu, Y. K. Wang, et al. 2010. Human lymphocyte antigen B-associated transcript 2, 3, and 5 polymorphisms and haplotypes are associated with susceptibility of Kawasaki disease and coronary artery aneurysm. J. Clin. Lab. Anal. 24:262–268.

Huang, I. C., C. C. Bailey, J. L. Weyer, S. R. Radoshitzky, M. M. Becker, J. J. Chiang, et al. 2011. Distinct patterns of IFITM-mediated restriction of filoviruses, SARS coronavirus, and influenza A virus. PLoS Pathog. 7:e1001258.

Jiang, D., J. M. Weidner, M. Qing, X. B. Pan, H. Guo, C. Xu, et al. 2010. Identification of five interferon-induced cellular proteins that inhibit west nile virus and dengue virus infections. J. Virol. 84:8332–8341.

Kato, H., T. Sugimura, T. Akagi, N. Sato, K. Hashino, Y. Maeno, et al. 1996. Long-term consequences of Kawasaki disease. A 10- to 21-year follow-up study of 594 patients. Circulation 94:1379–1385.

Kawasaki, T. 1979. Clinical signs and symptoms of mucocutaneous lymph node syndrome (Kawasaki disease). Jpn. J. Med. Sci. Biol. 32:237–238.

Kawasaki, T., F. Kosaki, S. Okawa, I. Shigematsu, and H. Yanagawa. 1974. A new infantile acute febrile mucocutaneous lymph node syndrome (MLNS) prevailing in Japan. Pediatrics 54:271–276.

Khor, C. C., S. Davila, W. B. Breunis, Y. C. Lee, C. Shimizu, V. J. Wright, et al. 2011. Genome-wide association study identifies FCGR2A as a susceptibility locus for Kawasaki disease. Nat. Genet. 43:1241–1246.

Kuo, H. C., Y. W. Hsu, C. M. Wu, S. H. Chen, K. S. Hung, W. P. Chang, et al. 2013. A replication study for association of ITPKC and CASP3 two-locus analysis in IVIG unresponsiveness and coronary artery lesion in Kawasaki disease. PLoS One 8:e69685.

Lehner, B., J. I. Semple, S. E. Brown, D. Counsell, R. D. Campbell, and C. M. Sanderson. 2004. Analysis of a high-throughput yeast two-hybrid system and its use to predict the function of intracellular proteins encoded within the human MHC class III region. Genomics 83:153–167.

Lu, J., Q. Pan, L. Rong, S. L. Liu, and C. Liang. 2011. The IFITM proteins inhibit HIV-1 infection. J. Virol. 85:2126–2137.

Martin, B. R., C. Wang, A. Adibekian, S. E. Tully, and B. F. Cravatt. 2012. Global profiling of dynamic protein palmitoylation. Nat. Methods 9:84–89.

Nakamura, Y., M. Yashiro, R. Uehara, A. Sadakane, S. Tsuboi, Y. Aoyama, et al. 2012. Epidemiologic features of Kawasaki

disease in Japan: results of the 2009–2010 nationwide
survey. J. Epidemiol. 22:216–221.

Ogata, S., A. H. Tremoulet, Y. Sato, K. Ueda, C. Shimizu, X.
Sun, et al. 2013. Coronary artery outcomes among children
with Kawasaki disease in the United States and Japan. Int. J.
Cardiol. 168:3825–3828.

Onouchi, Y. 2012. Genetics of Kawasaki disease: what we
know and don't know. Circ. J. 76:1581–1586.

Onouchi, Y., K. Ozaki, J. C. Buns, C. Shimizu, H. Hamada,
T. Honda, et al. 2010. Common variants in CASP3 confer
susceptibility to Kawasaki disease. Hum. Mol. Genet.
19:2898–2906.

Onouchi, Y., K. Ozaki, J. C. Burns, C. Shimizu, M. Terai,
H. Hamada, et al. 2012. A genome-wide association study
identifies three new risk loci for Kawasaki disease. Nat.
Genet. 44:517–521.

Rodriguez, S., T. R. Gaunt, and I. N. Day. 2009.
Hardy-Weinberg equilibrium testing of biological
ascertainment for Mendelian randomization studies.
Am. J. Epidemiol. 169:505–514.

Saji, T., and Y. Kemmotsu. 2006. Infliximab for Kawasaki
syndrome. J. Pediatr. 149:426.

Shulman, S. T., J. De Inocencio, and R. Hirsch. 1995.
Kawasaki disease. Pediatr. Clin. North Am. 42:1205–1222.

Smith, R. A., J. Young, J. J. Weis, and J. H. Weis. 2006.
Expression of the mouse fragilis gene products in immune
cells and association with receptor signaling complexes.
Genes Immun. 7:113–121.

Uehara, R., M. Yashiro, Y. Nakamura, and H. Yanagawa. 2004.
Clinical features of patients with Kawasaki disease whose
parents had the same disease. Arch. Pediatr. Adolesc. Med.
158:1166–1169.

Wang, C. L., Y. T. Wu, C. A. Liu, H. C. Kuo, and K. D. Yang.
2005. Kawasaki disease: infection, immunity and genetics.
Pediatr. Infect. Dis. J. 24:998–1004.

Weidner, J. M., D. Jiang, X. B. Pan, J. Chang, T. M. Block, and
J. T. Guo. 2010. Interferon-induced cell membrane proteins,
IFITM3 and tetherin, inhibit vesicular stomatitis virus
infection via distinct mechanisms. J. Virol. 84:12646–12657.

Zhang, Y. H., Y. Zhao, N. Li, Y. C. Peng, E. Giannoulatou,
R. H. Jin, et al. 2013. Interferon-induced transmembrane
protein-3 genetic variant rs12252-C is associated with severe
influenza in Chinese individuals. Nat. Commun. 4:1418.

Neil E. Bowles[1], Cammon B. Arrington[1], Keiichi
Hirono[2], Tsuneyuki Nakamura[3], Long Ngo[4], Yin Shen
Wee[5], Fukiko Ichida[2] and John H. Weis[5]
[1]*Division of Cardiology, Department of Pediatrics,
University of Utah School of Medicine, Salt Lake City, Utah*
[2]*Department of Pediatrics, Faculty of Medicine, University
of Toyama, Toyama, Japan*
[3]*Department of Pediatrics, Kanazawa Medical University,
Kanazawa, Japan*
[4]*Department of Medicine, Harvard Medical School, Beth
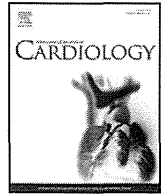Israel Deaconess Medical Center, Brookline, Massachusetts*
[5]*Department of Pathology, University of Utah School of
Medicine, Salt Lake City, Utah*

Correspondence
Neil E. Bowles, Department of Pediatrics (Cardiology), University of
Utah School of Medicine, Eccles Institute of Human Genetics, 15
North 2030 East, Room 7110B, Salt Lake City, UT 84112. Tel:
801-585-7574; Fax: 801-581-7404; E-mail: neil.bowles@hsc.utah.
edu

Letter to the Editor

Statin reduces persistent coronary arterial inflammation evaluated by serial ^{18}fluorodeoxyglucose positron emission tomography imaging long after Kawasaki disease

CrossMark

Kenji Suda [a,*], Nobuhiro Tahara [b], Akihiro Honda [b], Hironaga Yoshimoto [a], Shintaro Kishimoto [a], Yoshiyuki Kudo [a], Hayato Kaida [c], Toshi Abe [c], Takafumi Ueno [b], Yoshihiro Fukumoto [b]

[a] Department of Pediatrics and Child Health, Kurume University School of Medicine, Kurume, Japan
[b] Department of Cardiovascular Medicine, Kurume University School of Medicine, Kurume, Japan
[c] Department of Radiology, Kurume University School of Medicine, Kurume, Japan

We have recently reported a case with persistent coronary artery inflammation evaluated by ^{18}fluorodexoyglucose positron emission tomography (FDG-PET) long after the onset of Kawasaki disease (KD) for the first time [1] and here, we report the follow-up study 2 years after statin treatment.

The patient, 42-year-old male, suffered from KD at 4 month of age and left with giant left coronary artery aneurysm (CAA) and occluded giant right CAA. When he visited us at 40 years of age after long interval, a multi-detector X-ray computed tomography revealed persistent giant CAA at segment 6, stenosis distal to this CAA, persistent giant CAA at segment 11, and total occlusion of right coronary artery with collaterals from left coronary artery (Fig. 1). FDG-PET with co-registration of X-ray computed tomography showed significant FDG uptake around the left coronary orifice of the aortic wall and extending to the proximal left CAA wall with 1.48 of target-to-background ratio, indicating persistent inflammation (Fig. 2, upper panels). He has 2 atherogenic risk factors such as low concentrations of high-density lipoprotein (HDL) cholesterol and a history of smoking. After the initial evaluation of FDG-PET scan, he has been treated with 2 mg of pitavastatin and well without any events. Two years after the initiation of statin treatment, both C-reactive protein (0.22 mg/L at baseline to 0.164 mg/L on treatment) and low-density lipoprotein (LDL) cholesterol have decreased (1049 at baseline to 737 mg/L on treatment) though HDL cholesterol did not change significantly

(306 at baseline to 296 mg/L on treatment) and resultant LDL/HDL ratio decreased from 3.43 to 2.49. FDG-PET after 2-year statin treatment demonstrated the reduction of coronary inflammation with significantly smaller area and lower degree of FDG activity on the coronary wall with 1.28 of target-to-background ratio (Fig. 2, lower panels).

This case indicates that statin can reduce persistent coronary artery inflammation long after KD and FDG-PET can be a useful monitoring tool of this process. Though patients with a history of KD and residual CAA have known to have systemic inflammation [2] and statin may potentially alleviate systemic inflammation and improve endothelial function [3–5], there has been no data concerning change in local inflammation, notably coronary artery. Using FDG-PET, we could visually and quantitatively determine the coronary artery inflammation and demonstrated the reduction of coronary inflammation 2 years after statin treatment.

This is consistent with our previous report, in which we have shown that statin can attenuate local inflammation within thoracic and carotid artery plaques using FDG-PET [6]. Because this patient has few major atherogenic risk factors [7] and inflammation was exclusively localized at coronary aneurysmal wall, we thought this persistent coronary artery inflammation was directly related to KD itself.

This report further extends the application of FDG-PET for the evaluation of local vascular inflammation.

Disclosure

References

[1] K. Suda, N. Tahara, Y. Kudo, H. Yoshimoto, M. Iemura, T. Ueno, H. Kaida, M. Ishibashi, T. Imaizumi, Persistent coronary arterial inflammation in a patient long after the onset of Kawasaki disease, Int. J. Cardiol. 154 (2012) 193–194.
[2] Y. Mitani, H. Sawada, H. Hayakawa, K. Aoki, H. Ohashi, M. Matsumura, K. Kuroe, H. Shimpo, M. Nakano, Y. Komada, Elevated levels of high-sensitivity C-reactive protein and serum amyloid-A late after Kawasaki disease: association between inflammation and late coronary sequelae in Kawasaki disease, Circulation 111 (2005) 38–43.

* Corresponding author at: Department of Pediatrics and Child Health, Kurume University School of Medicine, Asahi-Machi 67, Kurume 830-0011, Japan.
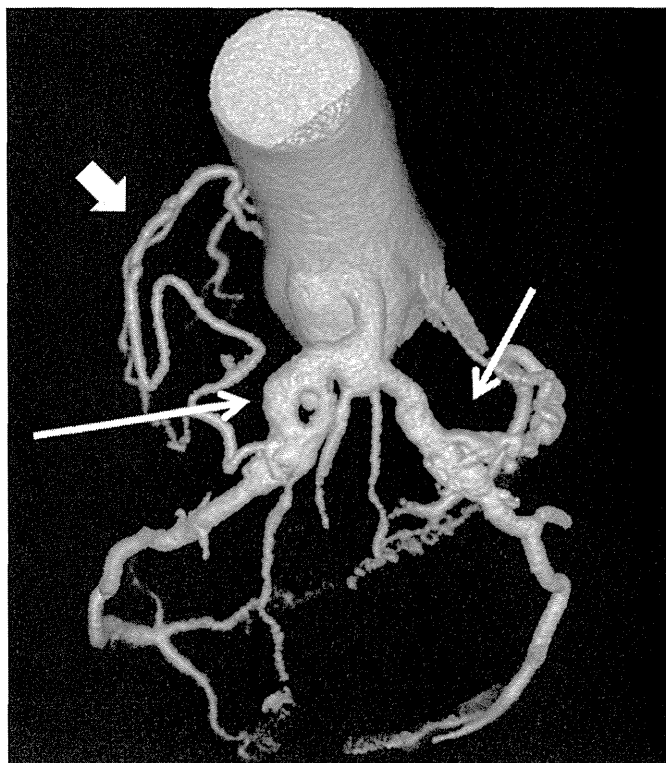E-mail address: suda_kenji@med.kurume-u.ac.jp (K. Suda).

Fig. 1. A multi-detector X-ray computed tomography revealed persistent giant coronary artery aneurysm (CAA) with 12 mm in diameter at segment 6 (white thin arrow), stenosis distal to this CAA, persistent giant CAA with 12 mm in diameter at segment 11 (white thin arrow), and total occlusion of right coronary artery with collaterals from left coronary artery (white thick arrow).

[3] S.M. Huang, K.P. Weng, J.S. Chang, W.Y. Lee, S.H. Huang, K.S. Hsieh, Effects of statin therapy in children complicated with coronary arterial abnormality late after Kawasaki disease: a pilot study, Circ. J. 72 (2008) 1583–1587.

[4] A. Hamaoka, K. Hamaoka, T. Yahata, M. Fujii, S. Ozawa, K. Toiyama, M. Nishida, T. Itoi, Effects of HMG-CoA reductase inhibitors on continuous post-inflammatory vascular remodeling late after Kawasaki disease, J. Cardiol. 56 (2010) 245–253.

[5] C. Duan, Z.D. Du, Y. Wang, L.Q. Jia, Effect of pravastatin on endothelial dysfunction in children with medium to giant coronary aneurysms due to Kawasaki disease, World J. Pediatr. 10 (2014) 232–237.

[6] N. Tahara, H. Kai, M. Ishibashi, H. Nakaura, H. Kaida, K. Baba, N. Hayabuchi, T. Imaizumi, Simvastatin attenuates plaque inflammation: evaluation by fluorodeoxyglucose positron emission tomography, J. Am. Coll. Cardiol. 48 (2006) 1825–1831.

[7] T.S. Noh, S.H. Moon, Y.S. Cho, S.P. Hong, E.J. Lee, J.Y. Choi, B.T. Kim, K.H. Lee, Relation of carotid artery 18F-FDG uptake to C-reactive protein and Framingham risk score in a large cohort of asymptomatic adults, J. Nucl. Med. 54 (2013) 2070–2076.
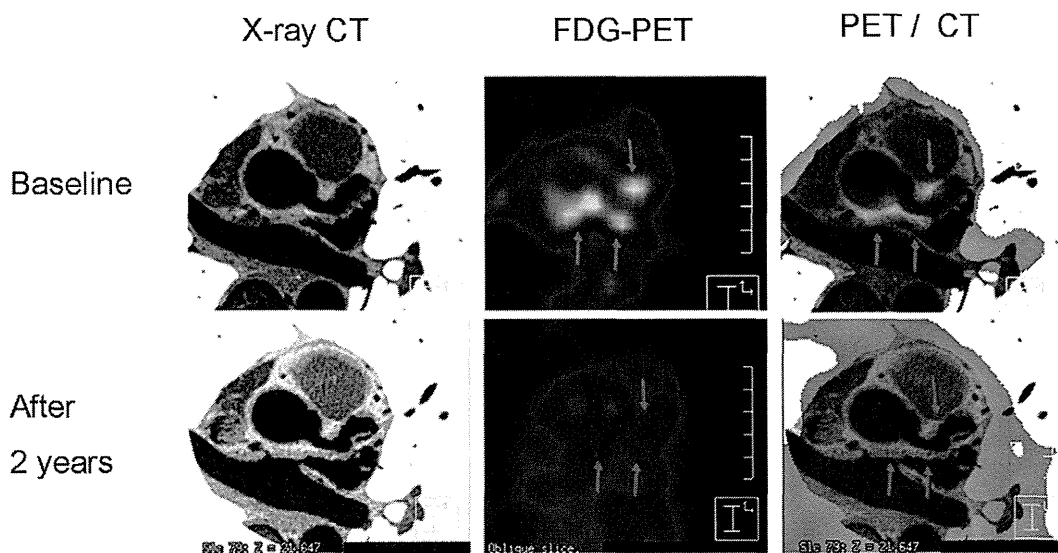
Fig. 2. Composite picture of PET/CT. From the left to right panel, X-ray computed tomography (X-ray CT), positron emission tomography using [18]fluorodexoyglucose (FDG-PET), and co-registered X-ray CT and FDG-PET were shown. Upper panels show baseline pictures and the bottom panels show pictures 2 years later. Statin treatment clearly alleviates the coronary inflammation with significantly smaller area and lower degree of FDG uptake.

Contents lists available at ScienceDirect

International Journal of Cardiology

CARDIOLOGY
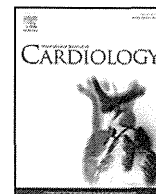
Letter to the Editor

Persistent peripheral arteritis long after Kawasaki disease — Another documentation of ongoing vascular inflammation

CrossMark

Kenji Suda [a,*], Nobuhiro Tahara [b], Akihiro Honda [b], Motofumi Iemura [a], Hironaga Yoshimoto [a],
Yoshiyuki Kudo [a], Hayato Kaida [c], Toshi Abe [c], Kentaro Sawada [d], Hidetoshi Akashi [d],
Hiroyuki Tanaka [d], Yoshihiro Fukumoto [b]

[a] Department of Pediatrics and Child Health, Kurume University School of Medicine, Kurume, Japan
[b] Department of Cardiovascular Medicine, Kurume University School of Medicine, Kurume, Japan
[c] Department of Radiology, Kurume University School of Medicine, Kurume, Japan
[d] Cardiovascular Surgery, Kurume University School of Medicine, Kurume, Japan

ARTICLE INFO

A 22-year-old male patient, who suffered from Kawasaki disease (KD) at 1 year and 1 month of age, treated with intravenous immunoglobulin infusion, but left with bilateral axillary arterial aneurysms and regressed coronary arterial aneurysms, presented with left hand edema and itchiness. He has been taking aspirin for thromboprophylaxis of axillary arterial aneurysms since the acute phase and well without any vascular events for these 20 years. He had no clinical evidence suggestive of Takayasu's or temporal arteritis, IgG4-related pathology, and autoimmune or collagen vascular disease. He was not obese with 20.4 kg/M^2 of body mass index and has resting blood pressure of 128/71 mm Hg on the right arm and 113/65 mm Hg on the left arm. Left hand was cold and showed clubbed fingers. Blood laboratory examination showed normal total cholesterol of 1790 mg/L, low-density lipoprotein cholesterol of 1020 mg/L, high-density-lipoprotein cholesterol of 771 mg/L and normal fasting glucose with glycosylated hemoglobin of 5.5%. The erythrocyte sedimentation rate of 2 mm/h and C-reactive protein of 0.04 mg/dL were normal.

* Corresponding author at: Department of Pediatrics and Child Health, Kurume University School of Medicine, Asahi-machi 67, Kurume 830-0011, Japan.
E-mail address: suda_kenji@med.kurume-u.ac.jp (K. Suda).

Digital subtraction angiography revealed complete occlusion of left axillary arterial aneurysm with multiple collateral arteries supplying blood flow to the distal arm (Fig. 1a) and a persistent giant right axillary arterial aneurysm with 12 mm in diameter with a proximal stenosis (Fig. 1b). To determine if the inflammatory activity was remaining in the axillary lesions, he underwent positron emission tomography using ^{18}F-fluorodeoxyglucose (FDG) [1,2] and multi-detector X-ray computed tomography. Positron emission tomography indeed demonstrated a focal FDG activity within the left axillary arterial aneurysm with 1.92 of target-to-background ratio and a lesser FDG activity at the mild stenotic site proximal to the right axillary arterial aneurysm with 1.84 of target-to-background ratio (Fig. 2).

Because he suffered from left arm ischemia, he underwent a resection of the left axillary arterial aneurysm and a successful axilla-brachial artery bypass surgery using a reversed autologous saphenous vein graft to relieve his symptoms. Macroscopic findings included multiple thrombi and calcified material occupying internal lumen of the axillary arterial aneurysm and heavily calcified internal wall. Histological examination of the resected wall showed an intimal thickening (Fig. 3a) and immunohistochemical analysis with CD68 antibody [3], as the marker of macrophages, revealed that magnitude of inflammation in the intimal thickening of the aneurysmal wall corresponded to the FDG activity (Fig. 3b).

This is the first documentation of persistent inflammation of peripheral arterial wall that can result in peripheral arterial remodeling long after KD. We have reported that coronary arterial aneurysms show progressive remodeling leading to obstructive lesion in patients with KD [4] and persisting coronary arteritis may be one of the underlying mechanisms [2]. In addition, inflammatory activity paralleled with the degree of vascular obstruction in this patient; the left axillary arterial aneurysm with complete obstruction demonstrated a higher degree of FDG activity than the right axillary arterial aneurysm with mild stenosis. Of note, FDG uptake was located exactly at the site of stenosis proximal to the right axillary arterial aneurysm. This can be the direct demonstration that local inflammatory activity leads to vascular remodeling.

In conclusion, peripheral arterial inflammation could persist long after KD leading to the vascular remodeling and positron emission tomography using FDG is a useful tool to detect local vascular inflammation.
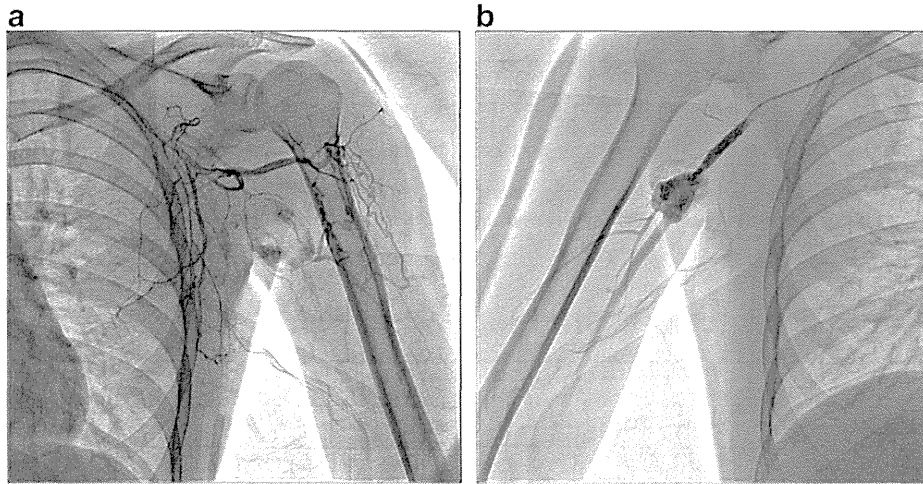
Fig. 1. Digital subtraction angiography revealed complete occlusion of left axillary arterial aneurysm with multiple collateral arteries supplying blood flow to the distal arm (a) and a persistent giant right axillary arterial aneurysm with 12 mm in diameter showing a proximal stenosis (b).
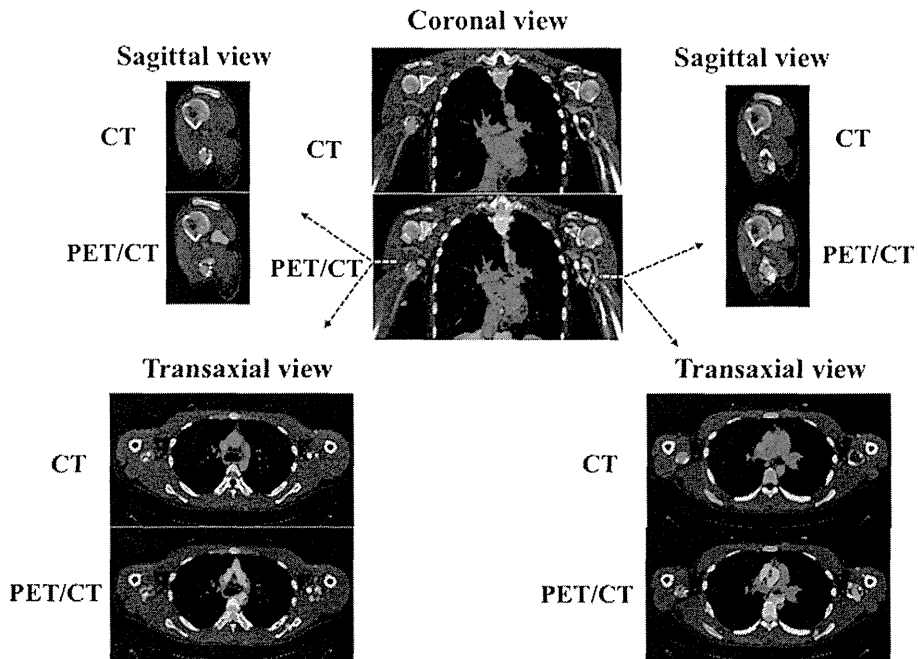

Fig. 2. The co-registration of multi-detector X-ray computed tomography of the left and right axillary arterial aneurysms and positron emission tomography using ^{18}F-fluorodeoxyglucose at the same plane showed a higher degree and larger area of FDG activity in the left axillary aneurysm than in the right axillary aneurysm.
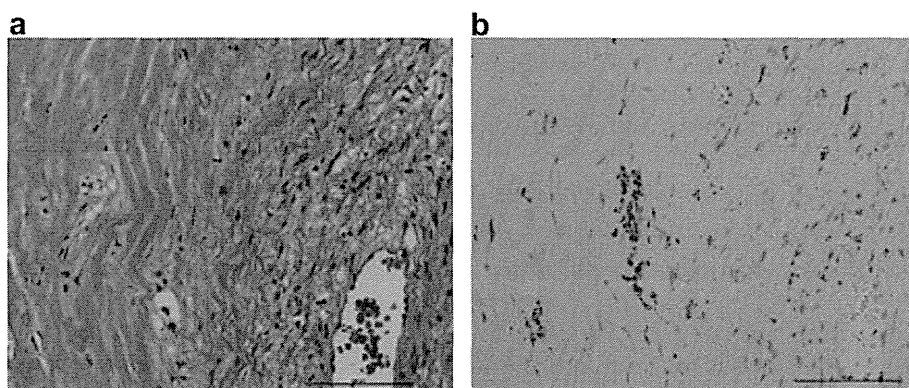

Fig. 3. Hematoxylin and eosin stain (×200 magnification) of the resected wall of the left axillary arterial aneurysm showed a proliferation of the intimal tissue (a). Immunohistochemical analysis with CD68 antibody (×200 magnification), as the marker of macrophages (brown color coded), revealed magnitude of inflammation in the intimal thickening of the aneurysmal wall corresponded to the fluorodeoxyglucose accumulation (b).

Conflict of interest

There was nothing to disclose and no conflict of interest among the authors.

References

[1] N. Tahara, T. Imaizumi, R. Virmani, J. Narula, Clinical feasibility of molecular imaging of plaque inflammation in atherosclerosis, J. Nucl. Med. 50 (2009) 331–334.

[2] K. Suda, N. Tahara, Y. Kudo, H. Yoshimoto, M. Iemura, T. Ueno, H. Kaida, M. Ishibashi, T. Imaizumi, Persistent coronary arterial inflammation in a patient long after the onset of Kawasaki disease, Int. J. Cardiol. 154 (2012) 193–194.

[3] A. Tawakol, R.Q. Migrino, G.G. Bashian, S. Bedri, D. Vermylen, R.C. Cury, D. Yates, G.M. LaMuraglia, K. Furie, S. Houser, H. Gewirtz, J.E. Muller, T.J. Brady, A.J. Fischman, In vivo 18F-fluorodeoxyglucose positron emission tomography imaging provides a noninvasive measure of carotid plaque inflammation in patients, J. Am. Coll. Cardiol. 48 (2006) 1818–1824.

[4] K. Suda, M. Iemura, H. Nishiono, Y. Teramachi, Y. Koteda, S. Kishimoto, Y. Kudo, S. Itoh, H. Ishii, T. Ueno, T. Tashiro, M. Nobuyoshi, H. Kato, T. Matsuishi, Long-term prognosis of patients with Kawasaki disease complicated by giant coronary aneurysms: a single-institution experience, Circulation 123 (2011) 1836–1842.